Electronic Supplementary Material (ESI) for Polymer Chemistry.
This journal is © The Royal Society of Chemistry 2018

Supporting information

Healing ionomer crosslinked by a *bis*-bidentate halogen bond linker: A way to hard and healable coatings

Jan Dahlke,[a,b] Ronny Tepper,[a,b] Robert Geitner,[c,d] Stefan Zechel,[a,b] Jürgen Vitz,[a,b] Robin Kampes,[a,b] Jürgen Popp,[b,c,d] Martin D. Hager,*[a,b] and Ulrich S. Schubert*[a,b]

[a] *Laboratory of Organic and Macromolecular Chemistry (IOMC), Friedrich Schiller University Jena, Humboldtstrasse 10, 07743 Jena (Germany), E-mail: ulrich.schubert@uni-jena.de; martin.hager@uni-jena.de*

[b] *Jena Center for Soft Matter (JCSM), Friedrich Schiller University Jena, Philosophenweg 7, 07743 Jena (Germany)*

[c] *Institute for Physical Chemistry and Abbe Center of Photonics (ACP), Friedrich Schiller University Jena, Helmholtzweg 4, 07743 Jena (Germany)*

[d] *Leibniz Institute for Photonic Technology (IPHT) Jena, Albert-Einstein-Strasse 9, 07745 Jena (Germany)*

Table of content:

1. Materials and instrumentation

All chemicals were used as purchased from Aldrich, ABCR, Acros, Fluka, Alfa Aesar and TCI without any further purification. The inhibitor from the commercially available monomer (butyl methacrylate) was removed by passing the liquid through a short aluminum oxide plug prior to use. Chloroform and dichloromethane were distilled before the use as eluent for Biobeads® column chromatography or reaction solvent. Furthermore, THF was dried by refluxing over sodium and benzophenone. For the purification *via* chromatography, silica gel 60 from Merck and BioBeads® S-X1 material from Bio-rad was used. The reaction progress was monitored by thin layer chromatography (TLC). For this purpose, aluminum sheets with precoated silica gel 60 F254 from Merck were used. The chemical shifts are reported in parts per million (ppm, δ scale) and the coupling constants are given in Hz.

The 1D (^{1}H, ^{13}C and ^{31}P) NMR spectra were measured on a Bruker AC 250 (250 MHz) and a Bruker AC 300 (300 MHz) at 298 K. For all spectra, the solvent was used as reference for the chemical shifts. The chemical shifts are reported in parts per million (ppm).

The elemental analyses were executed using a Euro EA 3000 (Heka Tech). The calculated values for the elemental analysis were based on the monomer composition and ratio (determined by titration) without endgroups.

For the DSC analysis a DSC 204 F1 Phoenix from Netzsch was used measuring under nitrogen atmosphere and with a heating rate of 10 and 20 K/min. The TGA measurements were performed with a Netzsch 449 F3 Jupiter (STA).

For the size exclusion chromatography measurements the following setup was utilized: A Shimadzu with a SCL-10A VP (system controller), a DGU-14A (degasser), a SIL-10AD VP (auto sampler), a RID-10A (RI detector), a LC-10AD VP (pump), a PSS GRAM guard/1000/30 Å (column), DMAc + 0.21% LiCl (eluent), 1 mL/min at 40 °C (flow rate and temperature) and poly(methyl methacrylate) standards.

All scratch healing experiments were performed on a polymer film. In order to prepare the films, 10 mg of the ionomer or the crosslinked networks were dissolved in 1 mL chloroform. The film was prepared *via* drop casting of 200 µL of the solution on the glass slide. The film was dried at room temperature and afterwards annealed for 20 h at 100 °C to remove the residual solvent.

The scratches on the film were cut with a feather disposable scalpel no. 11 (stainless steel) and all images were recorded with an optical microscope module of an atomic force microscopy (AFM) set up. The investigation of the healing behavior of the ionomer films was started at 100 °C. The glass slides were heated in an oven at the designated temperature for a specific time. If healing properties of the material were observable, the temperature and time for the healing process were reduced, until the scratches could not be healed anymore to identify the optimal healing conditions. The definition of a completely healed scratch is the full closure of the damaged surface. Samples defined as partial healing show no full recovery of the original surface but still show the tendency to close the crack. Lastly, materials, which are not able to close the area between the two sides of the scratch are considered as non-healing.

All ITC titrations were performed using a standard volume Nano ITC (TA Instruments) at 303 K. The solutions were always prepared prior to use in dry THF using vacuum dried hosts and guests. Bromide was added as tetrabutylammonium salt. Table S 7 shows the detailed experimental setup for each measurement including information about the concentration of host (H) and guest (G). Blank titrations in dry THF were performed and subtracted from the corresponding titrations to remove the effect of dilution. The fitting process was prepared with the NanoAnalyze program from TA instruments.

FT-Raman spectra were recorded up to 3600 cm^{-1} with a spectral resolution of 4 cm^{-1} using a Bruker MultiSpec spectrometer. A Nd:YAG laser (DeniCAFC-LC-3/40, Klastech-Karpushko Laser Technologies) provided the Raman excitation light at 1064 nm. The laser power was set to 1000 mW. The software package OPUS 6.5 was used to record the Raman spectra. Each spectrum consists of 512 single scans. The raw Raman spectra were pre-processed using R (3.3.2). The Raman spectra were restricted to the wavenumber region of interest, *i.e.*, the region between 180 and 3300 cm^{-1}. Subsequently, the Raman data were background corrected using a SNIP algorithm (iterations = 100, order = 2, smoothing window = 3). In the end the Raman spectra were vector normalized.

2. Experimental section

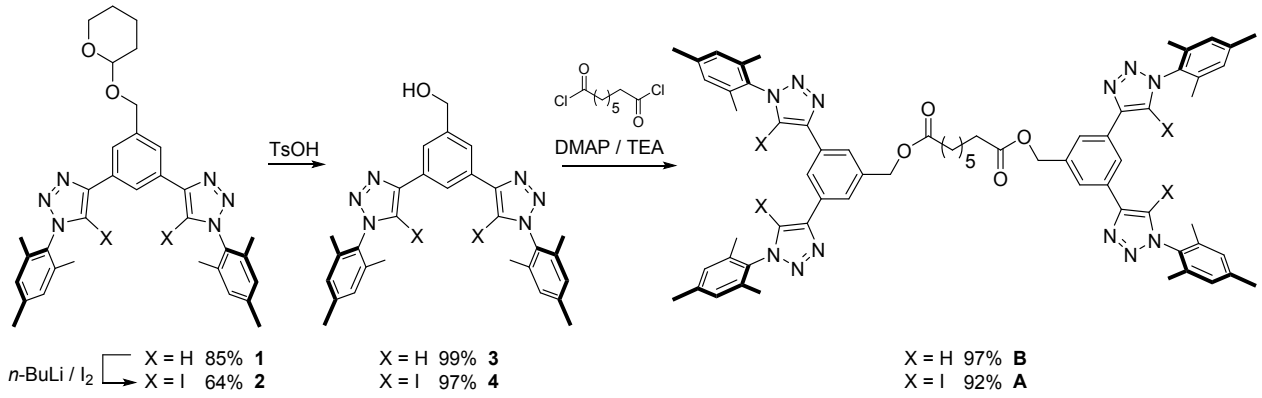

Scheme S 1: Schematic representation of the synthesis of HB- and XB-based bis-bidentate receptors.

The substances **1** to **4** were synthesized as described in literature.[1]

General procedure for the reaction of dichloride with benzyl alcohols

A 25 mL two-neck round-bottom flask was charged with the benzyl alcohol derivative educt (2.3 eq.) dissolved in dry CH_2Cl_2 under a nitrogen atmosphere. Successively, 4-dimethylamino-pyridine (DMAP, 0.4 eq.) and triethylamine (TEA, 2.3 eq.) were added. After stirring for 15 min at room temperature, octanedioyl dichloride (1 eq.) was added dropwise and stirred for additional 2 h, whereupon the solution became turbid. The mixture was extracted with CH_2Cl_2 and water, the organic fraction was dried over sodium sulfate, filtered, and was concentrated *in vacuo*. The crude product was purified by flash column chromatography (silica, CH_2Cl_2 to CH_2Cl_2/methanol (99:1)) to obtain the desired products as white solids.

***Bis*(3,5-*bis*(5-iodo-1-mesityl-1*H*-1,2,3-triazol-4-yl)benzyl) octanedioate (A)**

Following the general procedure, **4** (175 mg, 0.24 mmol), DMAP (5.1 mg, 0.04 mmol), tri-ethylamine (33 µL, 0.24 mmol) and commercially available octanedioyl dichloride (22 mg, 19 µL, 0.11 mmol) were allowed to react in 6 mL dry CH_2Cl_2 for 2 h at room temperature to yield the desired product **A** (154 mg, 92%). ^{1}H NMR (300 MHz, $CDCl_3$) δ = 8.83 (s, 2H), 8.18 (s, 4H), 7.05 (s, 8H), 5.28 (s, 4H), 2.47 – 2.41 (m, 4H), 2.39 (s, 12H), 1.96 (s, 24H), 1.74 – 1.62 (m, 4H), 1.41 – 1.32 (m, 4H) ppm; ^{13}C NMR (75 MHz, $CDCl_3$) δ = 173.7, 149.0, 140.9, 137.3, 136.0, 133.1, 131.1, 129.3, 127.1, 125.5, 80.1, 65.9, 34.3, 28.9, 24.9, 21.4, 17.7 ppm; HRMS (*m/z*): $[M + Na^+]^+$ calcd. for $C_{66}H_{66}I_4N_{12}O_4Na$ 1621.1401, found 1621.1346.

***Bis*(3,5-*bis*(1-mesityl-1*H*-1,2,3-triazol-4-yl)benzyl) octanedioate (B)**

Following the general procedure, **3** (400 mg, 0.84 mmol), DMAP (17.8 mg, 0.15 mmol), triethylamine (116 µL, 0.84 mmol) and commercially available octanedioyl dichloride (77 mg, 66 µL, 0.36 mmol) were allowed to react in 5 mL dry CH_2Cl_2 for 2 h at room temperature to yield the desired product **B** (386 mg, 97%). ^{1}H NMR (300 MHz, $CDCl_3$) δ = 8.40 (s, 2H), 7.97 (s, 4H), 7.94 (s, 4H), 6.99 (s, 8H), 5.20 (s, 4H), 2.41 – 2.35 (m, 4H), 2.34 (s, 12H), 1.99 (s, 24H), 1.72 – 1.57 (m, 4H), 1.40 – 1.27 (m, 4H) ppm; ^{13}C NMR (75 MHz, $CDCl_3$) δ = 173.6, 146.9, 140.2, 137.7, 135.0, 133.4, 131.6, 129.2, 125.2, 122.8, 122.2, 65.8, 34.2, 28.8, 24.7, 21.2, 17.4 ppm; HRMS (*m/z*): $[M + Na^+]^+$ calcd. for $C_{66}H_{70}N_{12}O_4Na$ 1117.5535, found 1117.5499.

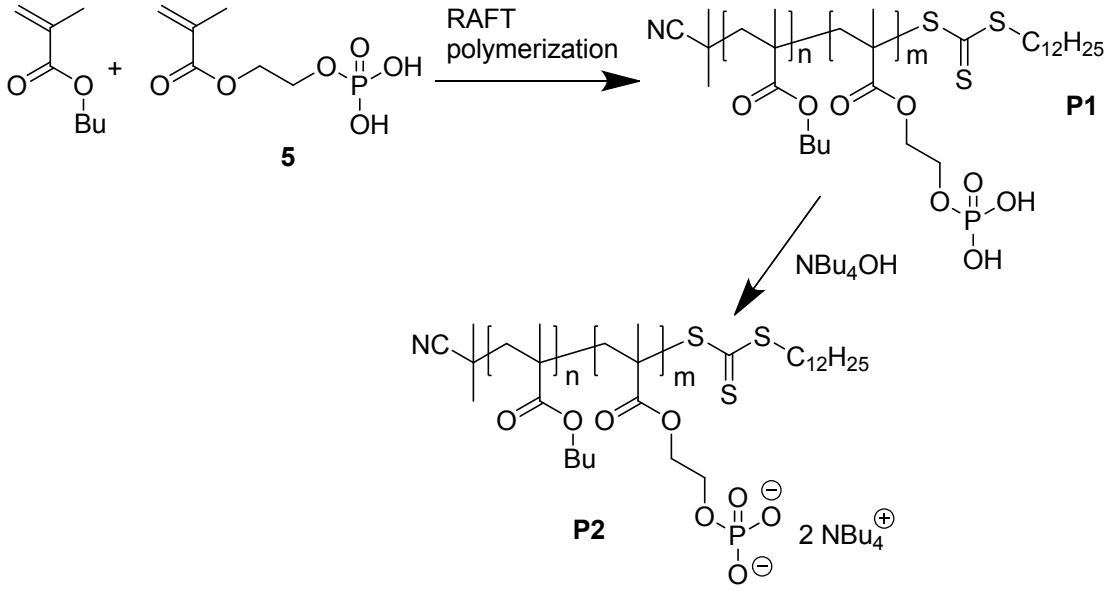

*Scheme S 2: Schematic representation of the synthesis copolymer **P1** and ionomer **P2**.*

MOEP (5)

The synthesis procedure of 2-(methacryloyloxy)ethyl phosphate (MOEP, **5**) was performed according to literature procedures.[2]

Synthesis of the copolymer P1

In order to perform the RAFT polymerizations, a suitable microwave vial or flask was utilized for the reaction. All monomers (**5**, butyl methacrylate (BMA)) were dissolved in the required amount of dry dimethylformamide. Subsequently, the initiator (AIBN) and the chain transfer agent (CTA) were added by calculated volumes from freshly prepared stock solutions. As CTA

2-cyano-2-propyl dodecyl trithiocarbonate (CPDT) was utilized. The reaction mixture was purged with nitrogen for 30 min through the septa of the closed vial or flask prior to the start of the reaction. Afterwards, the solution was placed in an oil bath with stirrer, preheated to the required temperature.

For the copolymerization, a 4:1 ratio of CTA to AIBN was utilized. The ratio of monomer to CTA was 150/1. All additional reaction details are listed in Table S 1 below. The polymers were purified by BioBeads® column chromatography (S-X1, swollen in chloroform).

Table S 1: Summary of the details for the RAFT polymerization.

Sample	Monomers	CTA	m (monomers) [mg]	m (AIBN) [mg]	m (CTA) [mg]	V (DMF) [mL]	Time [h]	T [°C]
P1	**5** BMA	CPDT	821 5,000	10.7	90.0	19.5	17	80

^{1}H NMR (400 MHz, $CDCl_3$) δ = 4.24 (s, 0.2H), 3.94 (s, 1H), 2.84 (s, 0.05H), 2.14 – 0.69 (m, 5.65H) ppm; ^{31}P NMR (250 MHz, $CDCl_3$): δ = 0.96 ppm; elemental analysis: calcd. C: 62.88%, H: 9.27%, N: -, found: C: 63.09%, H: 9.34%, N: 0.29%.

Synthesis of the ionomer P2

1.035 g of the neutral copolymer **P1** was placed in a vial and dissolved in the required amount of chloroform. After the complete dissolution of the polymer, 0.85 mL of NBu_4OH (37% in methanol) was added dropwise to the solution. The reaction mixture was stirred for several minutes at room temperature. Subsequently, the solvent was removed *in vacuo* and the product was dried thoroughly.

^{1}H NMR (400 MHz, $CDCl_3$) δ = 3.95 (s, 1H), 3.38 (s, 0.56H), 2.51 – 2.26 (m, 0.08H), 2.13 – 0.70 (m, 7.48H) ppm; ^{31}P NMR (250 MHz, $CDCl_3$): δ = 1.11 ppm; elemental analysis, calcd.: C: 65.27%, H: 9.96%, N: 0.80%, found: C: 63.85%, H: 10.24%, N: 1.28%.

Synthesis of the crosslinked networks

The exact amounts of the ionomer **P2** and the XB- (**A**) or HB-based (**B**) linker were dissolved in chloroform and combined. Afterwards, the solvent was removed *in vacuo* and the polymer was dried. For the calculation of the masses for the reaction, a ratio of 1:2 (linker/phosphate groups) was applied. A summary of the reaction details is shown in Table S 2.

Table S 2: Summary of the details for the synthesis of the crosslinked ionomer networks.

Sample	Polymer	Linker	m (polymer) [mg]	m (linker) [mg]
P2A	**P2**	**A**	52.5	21.1
P2B	**P2**	**B**	49.3	13.5
P1A	**P1**	**A**	23.3	12.3

Table S 3: Summarized thermal properties of the polymers and polymer networks determined by DSC.

Ionomer	Linker	T_g [°C]	T_d [°C]
P1	–	44.0	217
P2	–	33.3	224
P1A	**A**	41.5	212
P2A	**A**	35.3	229
P2B	**B**	–[a)]	231

[a)] no T_g detectable.

3. Size-exclusion chromatography (SEC)

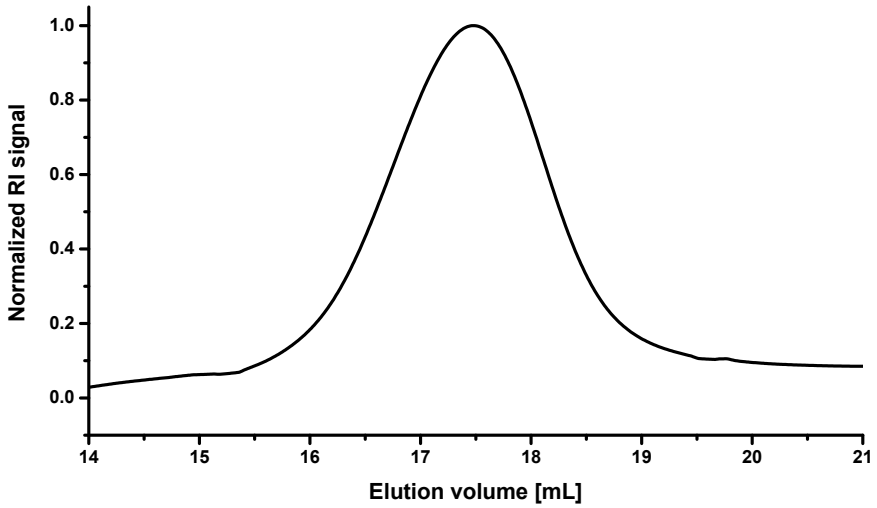

*Figure S 1: SEC curve of **P1**, eluent DMAc/LiCl, PMMA as standard.*

*Table S 4: SEC results for polymer **P1**.*

Polymer	M_n [g/mol]	M_w [g/mol]	Đ
P1	15,100	18,200	1.21

The values for **P1** are considered as valid as well for ionomer **P2** and the crosslinked networks **P1A**, **P2A** and **P2B**. The determination of the molar mass of the ionomer and the crosslinked networks, respectively, is not possible *via* SEC because of the network formation.

4. Acid-base titration

In order to determine the content of acid groups within the copolymer, the following titration method was established. In an Erlenmeyer flask, the neutral copolymer was weighed in, dissolved in THF and two drops of phenolphthalein solution (0.1 M in ethanol) were added. Subsequently, the colorless solution was titrated with KOH solution (0.05 M in ethanol) until a color change from colorless to pink was observed. The monomer MOEP (**5**) and the resulting functional phosphate containing unit in the copolymer can be deprotonated twice and was, therefore, titrated with a stoichiometry of two. The titration was performed three times and the average value of the content was utilized for further calculations.

*Table S 5: Titration results of the neutral copolymer **P1**.*

Polymer	Monomer A/B	Calculated ratio [A]/[B]	Calculated content of MOEP (5)
P2	BMA/MOEP (**5**)	9.1/1	9.9%

5. Differential scanning calorimetry (DSC)

P1

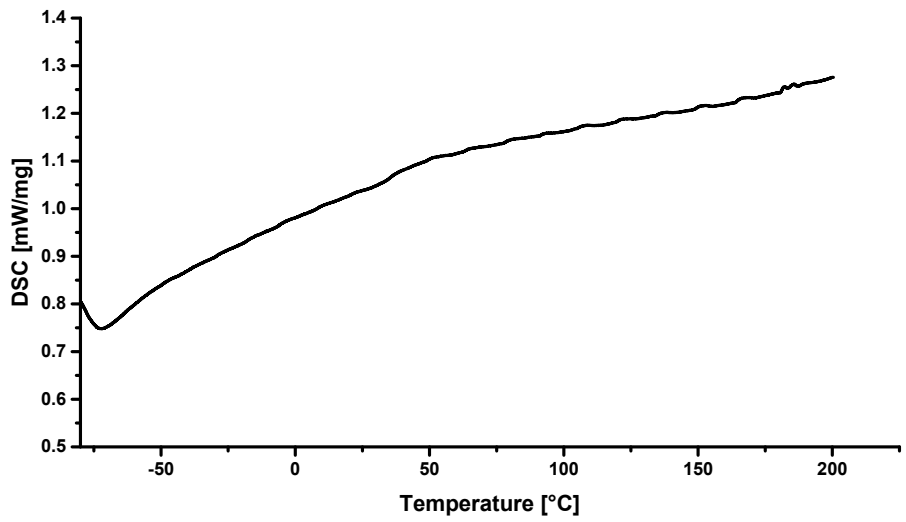

*Figure S 2: DSC curve of **P1**. 2nd Heating curve 20 K/min, –100 to 200 °C.*

P2

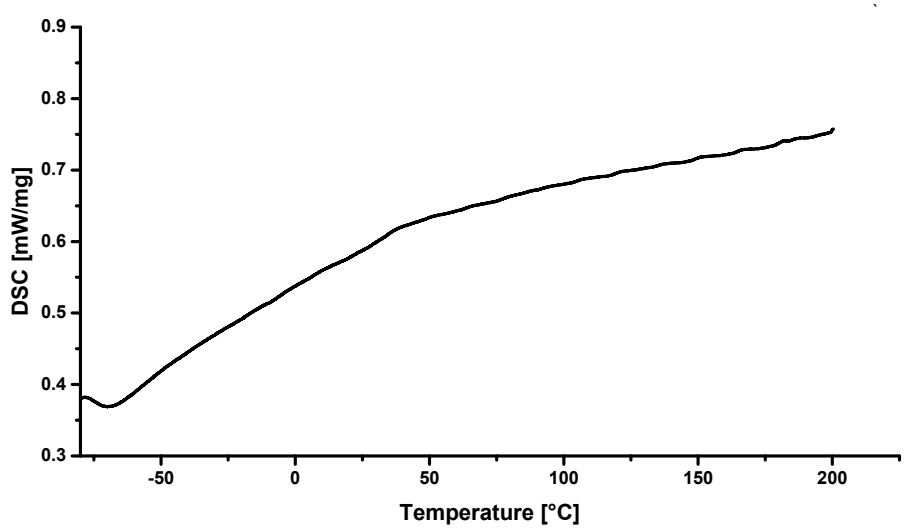

*Figure S 3: DSC curve of **P2**. 2nd Heating curve 20 K/min, –100 to 200 °C.*

P2A

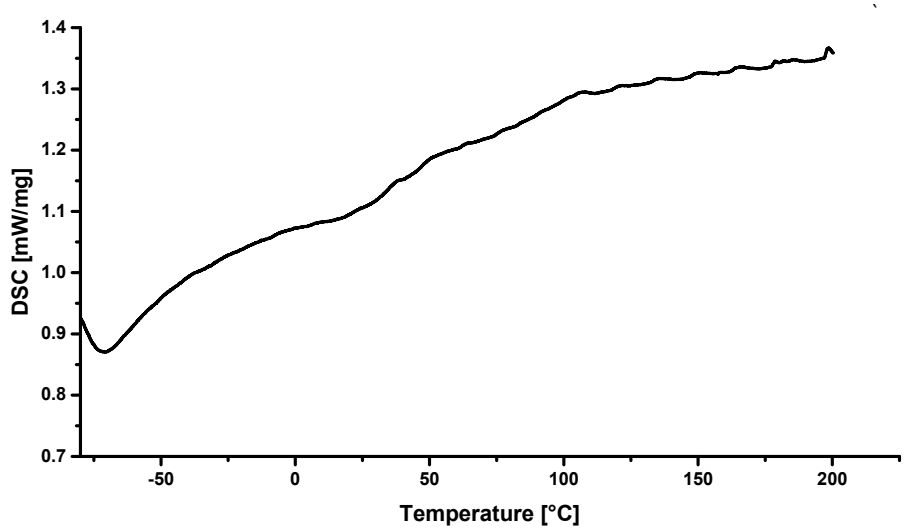

*Figure S 4: DSC curve of **P2A**. 2nd Heating curve 20 K/min, –100 to 200 °C.*

P2B

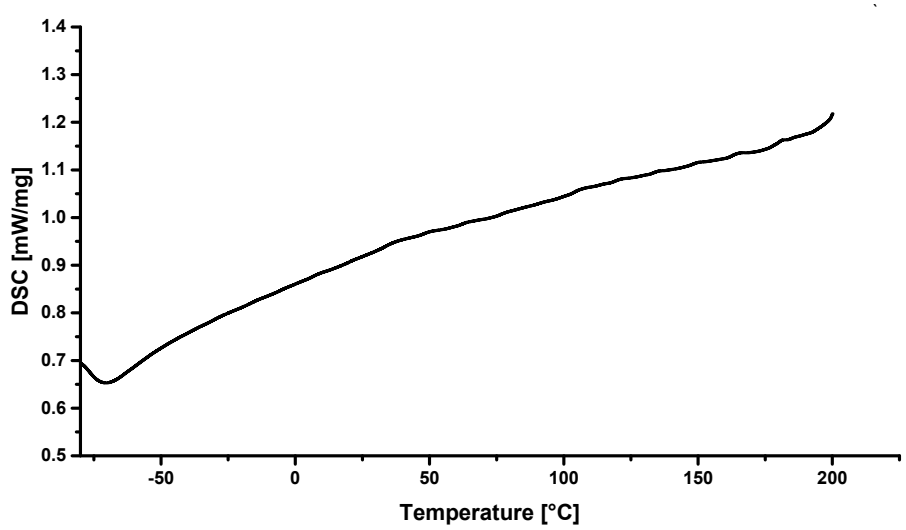

*Figure S 5: DSC curve of **P2B**. 2nd Heating curve 20 K/min, –100 to 200 °C.*

P1A

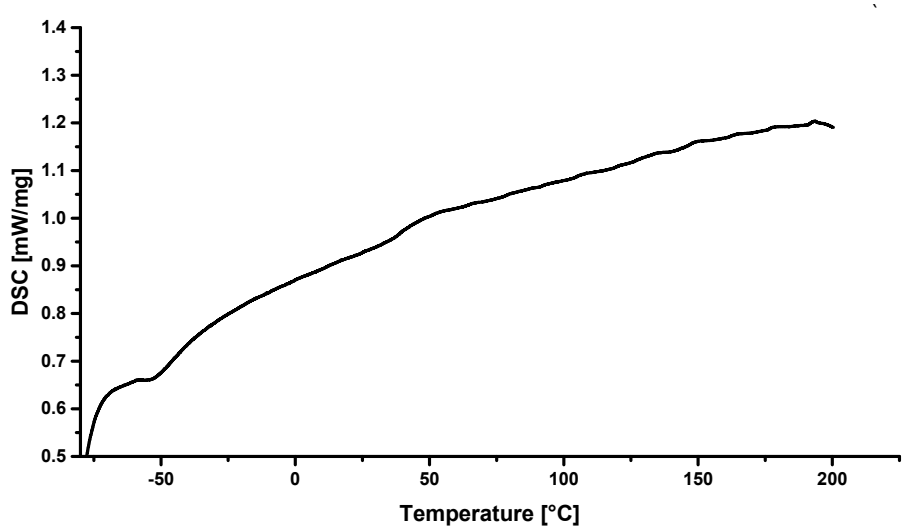

*Figure S 6: DSC curve of **P1A**. 2nd Heating curve 20 K/min, –100 to 200 °C.*

6. Thermal gravimetric analysis (TGA)

P1

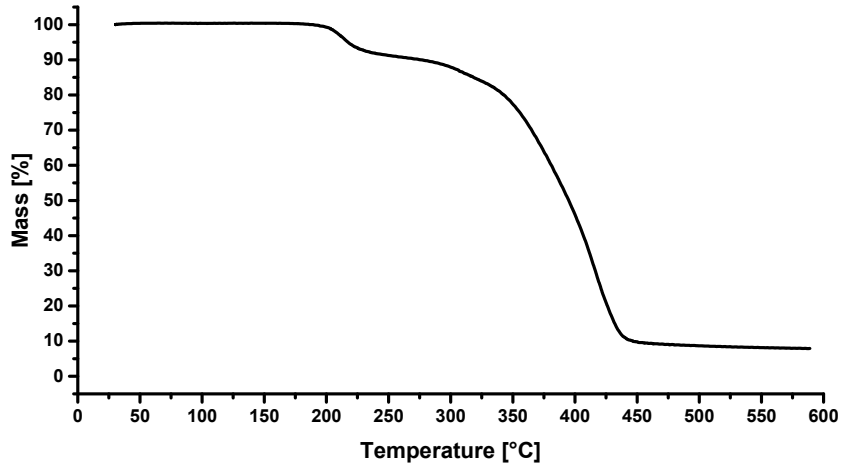

*Figure S 7: TGA measurement of **P1**. Heating rate 20 K/min; heating from 20 to 590 °C.*

P2

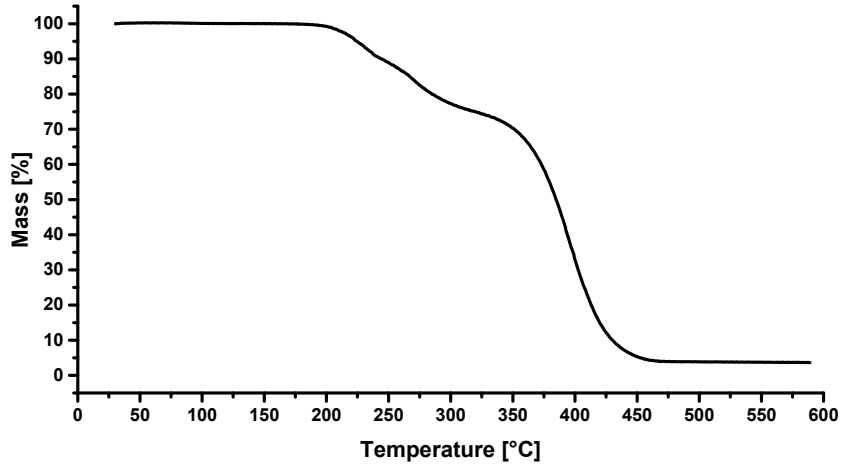

*Figure S 8: TGA measurement of **P2**. Heating rate 20 K/min; heating from 20 to 590 °C.*

P1A

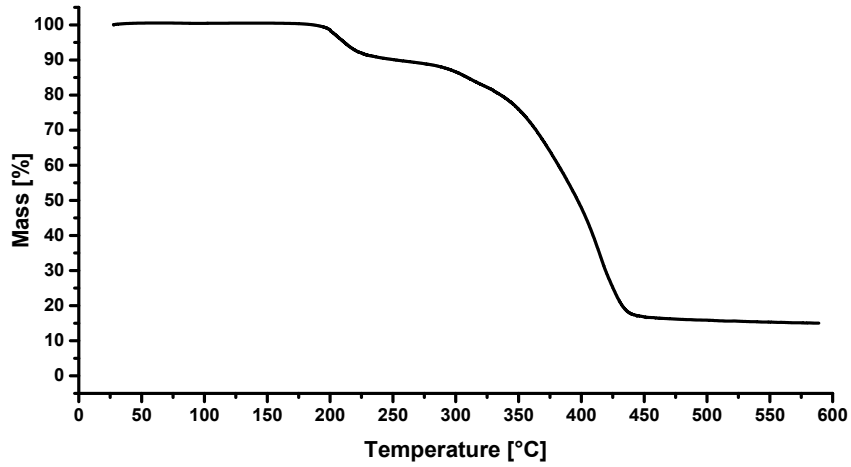

*Figure S 9: TGA measurement of **P1A**. Heating rate 20 K/min; heating from 20 to 590 °C.*

P2A

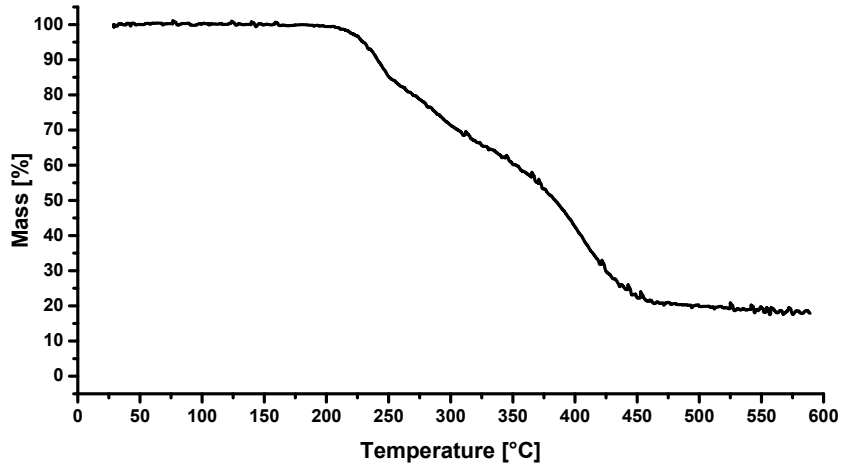

*Figure S 10: TGA measurement of **P2A**. Heating rate 20 K/min; heating from 20 to 590 °C.*

P2B

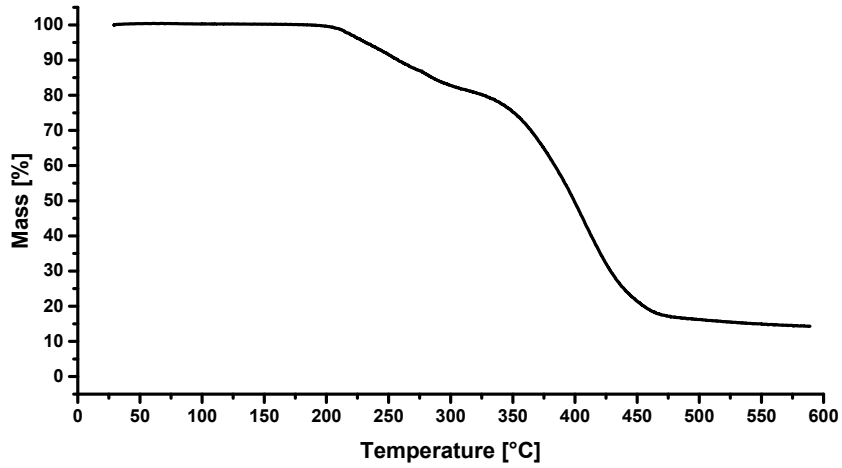

*Figure S 11: TGA measurement of **P2B**. Heating rate 20 K/min; heating from 20 to 590 °C.*

7. NMR spectroscopy

Linker A

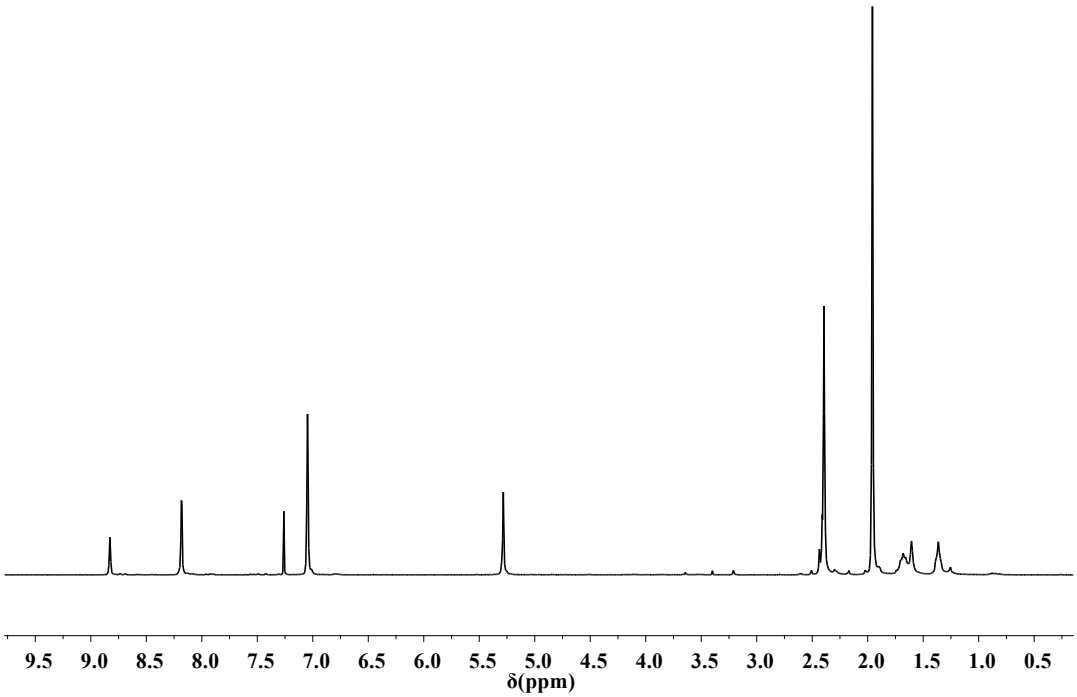

*Figure S 12: [1]H NMR of **A**, $CDCl_3$ (300 MHz).*

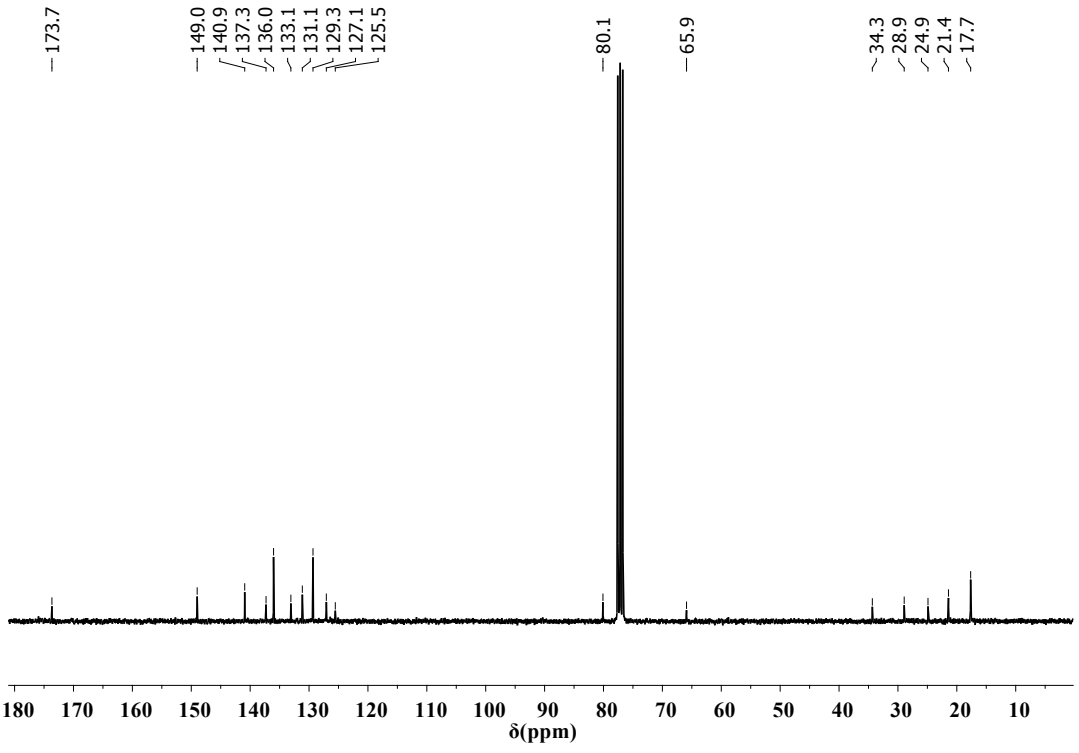

*Figure S 13: [13]C NMR of **A**, $CDCl_3$ (75 MHz).*

Linker B

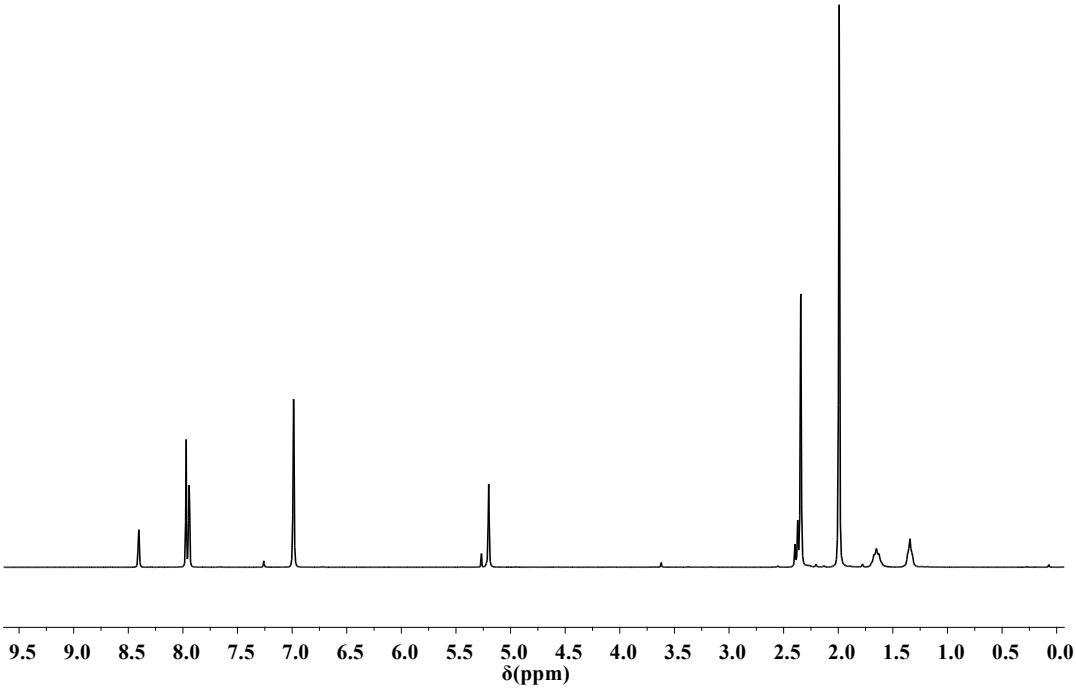

*Figure S 14: [1]H NMR of **B**, $CDCl_3$ (300 MHz).*

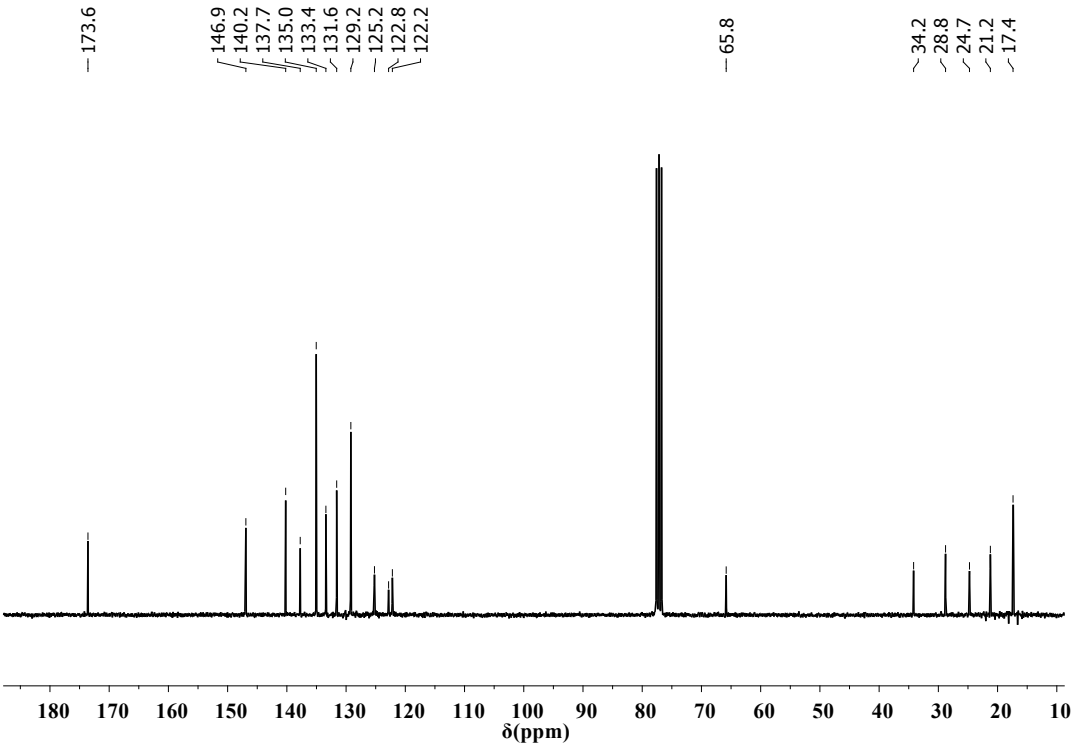

*Figure S 15: [13]C NMR of **B**, $CDCl_3$ (75 MHz).*

P1

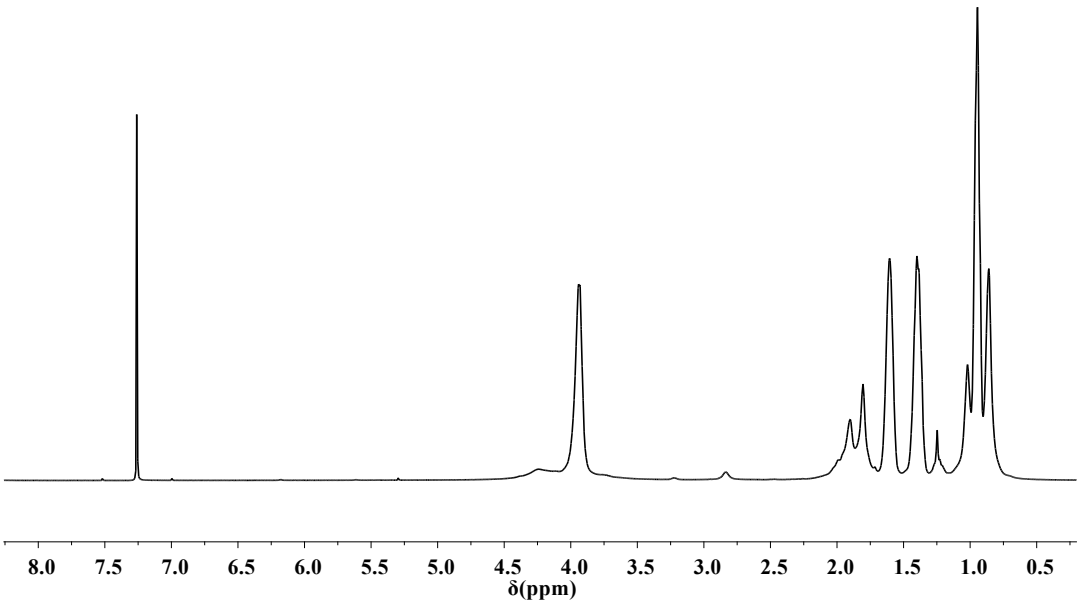

*Figure S 16: ^1H NMR of **P1**, $CDCl_3$ (300 MHz).*

P2

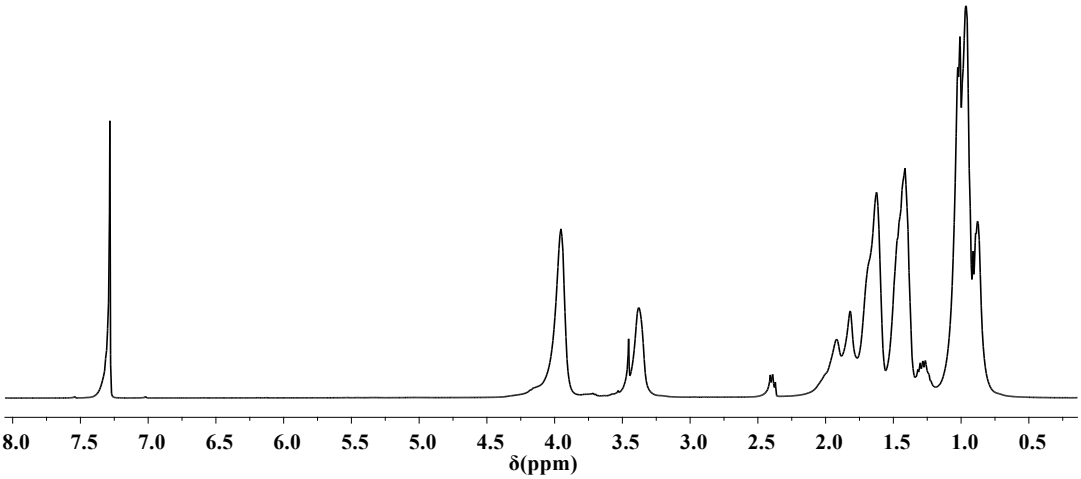

*Figure S 17: ^1H NMR of **P2**, $CDCl_3$ (300 MHz).*

8. Raman spectroscopy

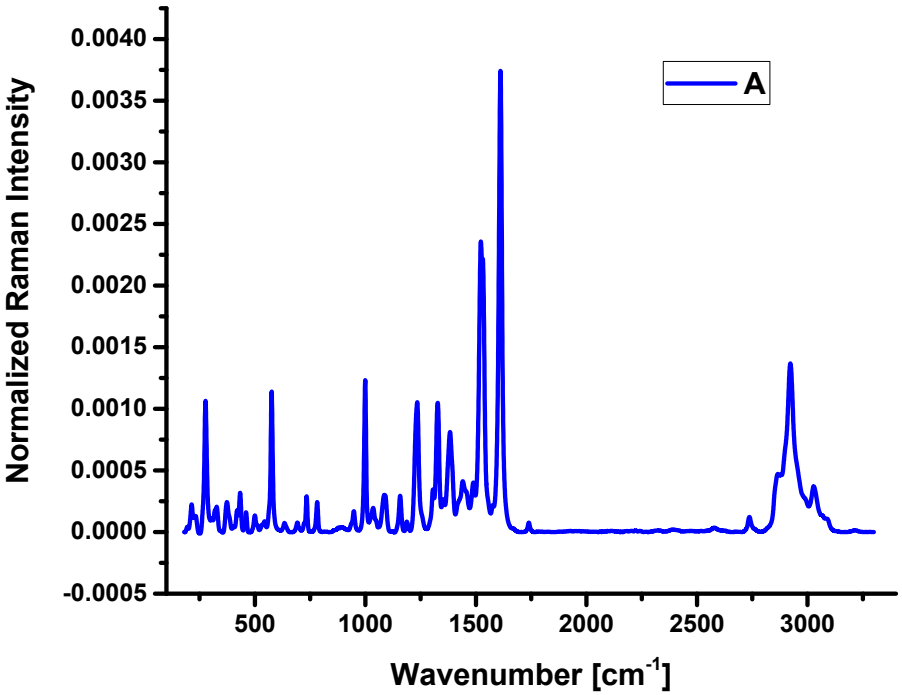

*Figure S 18: Raman spectrum of the linker **A**. Band assignment 3090 (vw, ν(=C-H)), 3067 (vw, ν(=C-H)), 3029 (vw, ν(=C-H)), 2990 (vw, ν(C-H)), 2922 (w, ν(C-H)), 2900 (vw, ν(C-H)), 2878 (vw, ν(C-H)), 2865 (vw, ν(C-H)), 2737 (vw, ν(C-H)), 1740 (vw, ν(C=O)), 1612 (vs, ν(C=C)), 1576 (vw, ν(C=C)), 1531 (m, ν(C=C)), 1524 (s, ν(C=C)), 1488 (sh, δ(C-H)), 1457 (vw, δ(C-H)), 1440 (sh, δ(C-H)), 1418 (vw), 1383 (w), 1353 (vw), 1327 (w), 1306 (vw), 1234 (w), 1187 (vw), 1157 (vw), 1087 (vw), 1048 (vw), 1036 (vw), 999 (w, ring breath phenyl), 948 (vw), 782 (vw), 734 (vw), 723 (vw), 693 (vw), 634 (vw), 576 (w, ring breath mesityl), 544 (vw), 534 (vw), 511 (vw), 501 (vw), 460 (vw), 433 (vw), 420 (vw), 385 (vw), 374 (vw), 328 (vw), 318 (vw), 306 (vw), 277 (w, ν(C-I)), 232 (vw), 214 (vw), 194 (vw) cm^{-1}.*

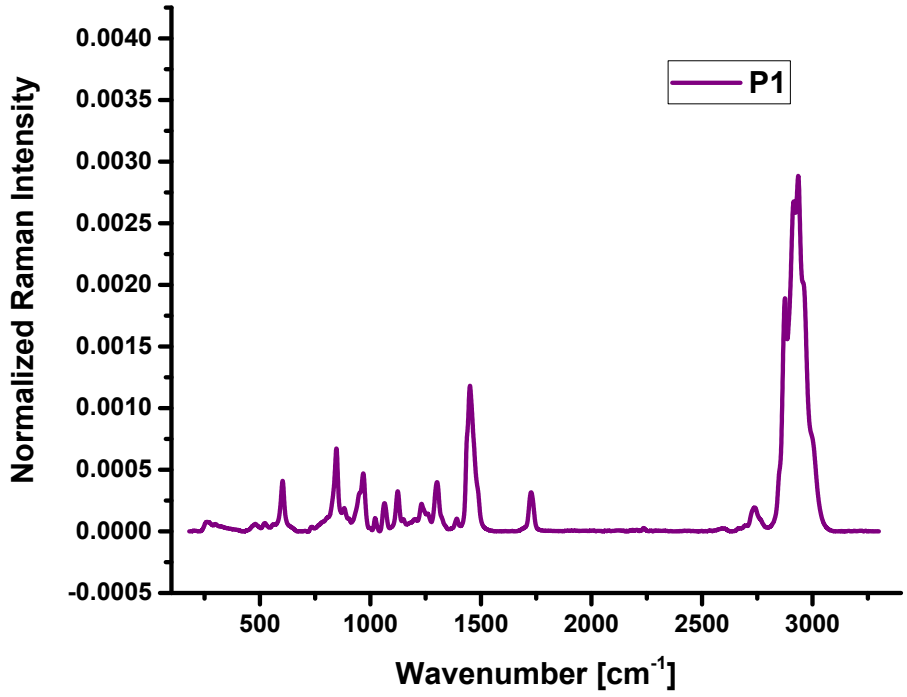

Figure S 19: *Raman spectrum of the polymer **P1**. Band assignment 2999 (w, ν(C-H)), 2958 (s, ν(C-H)), 2935 (vs, ν(C-H)), 2915 (vs, ν(C-H)), 2875 (s, ν(C-H)), 2852 (vw, ν(C-H)), 2739 (vw, ν(C-H)), 1727 (vw, ν(C=O)), 1484 (sh, δ(C-H)), 1450 (m, δ(C-H)), 1438 (sh), 1390 (vw), 1301 (vw), 1260 (vw), 1231 (vw), 1200 (vw), 1149 (vw), 1124 (vw), 1064 (vw), 1022 (vw), 968 (vw), 950 (vw), 902 (vw), 883 (vw), 846 (w), 735 (vw), 603 (vw), 559 (vw), 522 (vw), 479 (vw), 299 (vw), 259 (vw) cm^{-1}.*

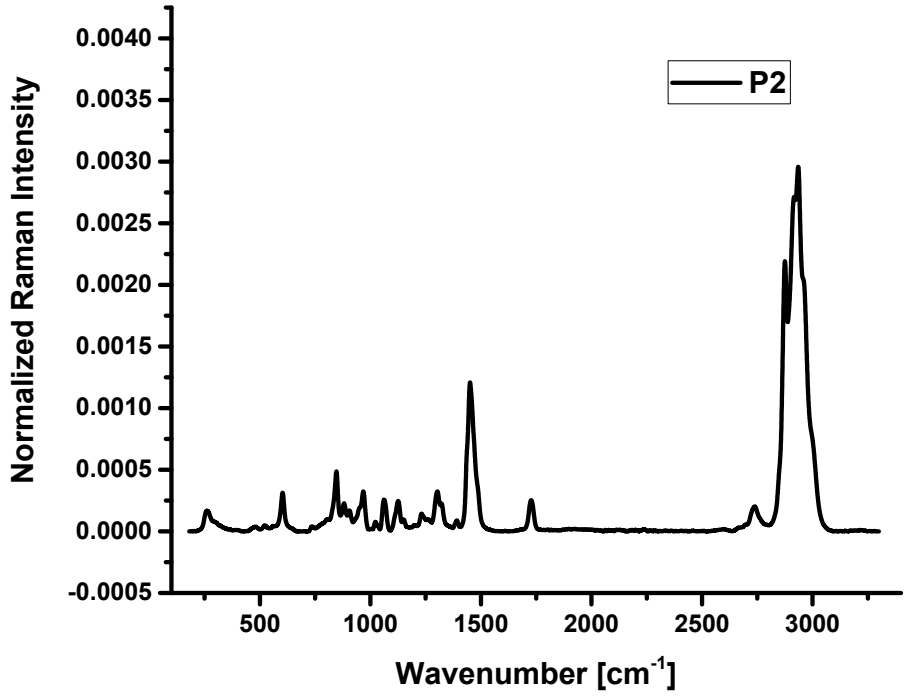

Figure S 20: *Raman spectrum of the polymer **P2**. Band assignment 2994 (w, ν(C-H)), 2959 (s, ν(C-H)), 2935 (vs, ν(C-H)), 2917 (vs, ν(C-H)), 2875 (s, ν(C-H)), 2852 (vw, ν(C-H)), 2738 (vw, ν(C-H)), 1727 (vw, ν(C=O)), 1485 (sh, δ(C-H)), 1451 (m, δ(C-H)), 1438 (sh), 1390 (vw), 1322 (vw), 1302 (vw), 1260 (vw), 1231 (vw), 1200 (vw), 1151 (vw), 1126 (vw), 1110 (vw), 1063 (vw), 1034 (vw), 1023 (vw), 968 (vw), 949 (vw), 905 (vw), 880 (vw), 846 (vw), 805 (vw), 737 (vw), 603 (vw), 561 (vw), 522 (vw), 478 (vw), 261 (vw) cm^{-1}.*

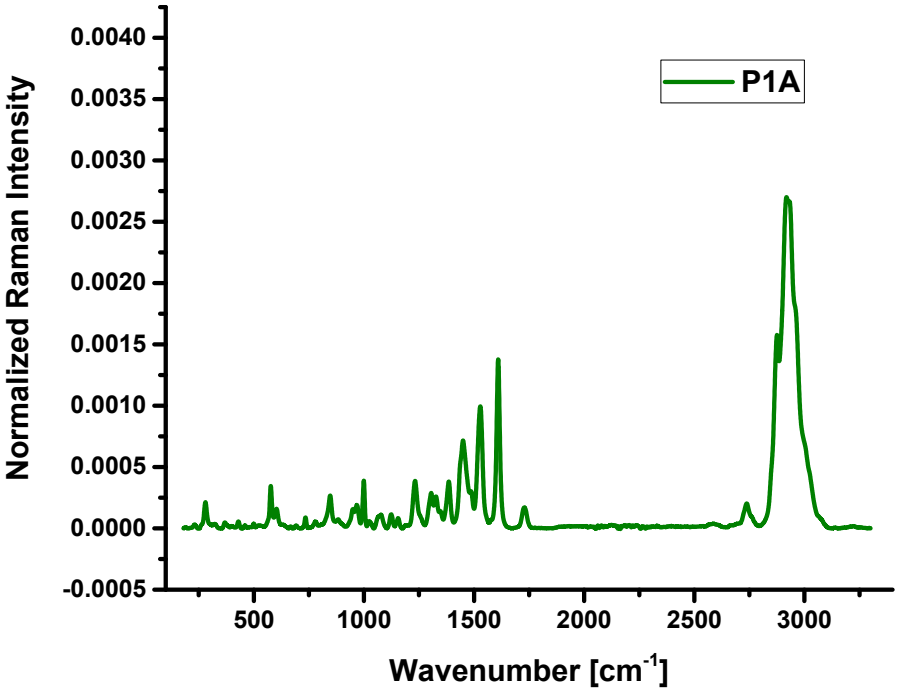

*Figure S 21: Raman spectrum of the polymer **P1A.** Band assignment 3071 (sh, ν(=C-H)), 3024 (sh, ν(=C-H)), 2998 (sh, ν(C-H)), 2959 (s, ν(C-H)), 2933 (vs, ν(C-H)), 2918 (vs, ν(C-H)), 2876 (m, ν(C-H)), 2738 (vw, ν(C-H)), 1728 (vw, ν(C=O)), 1609 (m, ν(C=C)), 1576 (vw, ν(C=C)), 1529 (w), 1487 (vw, δ(C-H)), 1450 (w, δ(C-H)), 1440 (sh, δ(C-H)), 1386 (vw), 1348 (vw), 1327 (vw), 1306 (vw), 1257 (sh), 1232 (vw), 1156 (vw), 1124 (vw), 1077 (vw), 1065 (vw), 1024 (vw), 1000 (vw, ring breath phenyl), 968 (vw), 950 (vw), 883 (vw), 847 (vw), 779 (vw), 735 (vw), 693 (vw), 668 (vw), 604 (vw), 577 (vw, ring breath mesityl), 500 (vw), 460 (vw), 429 (vw), 369 (vw), 322 (vw), 280 (vw), 231 (vw) cm^{-1}.*

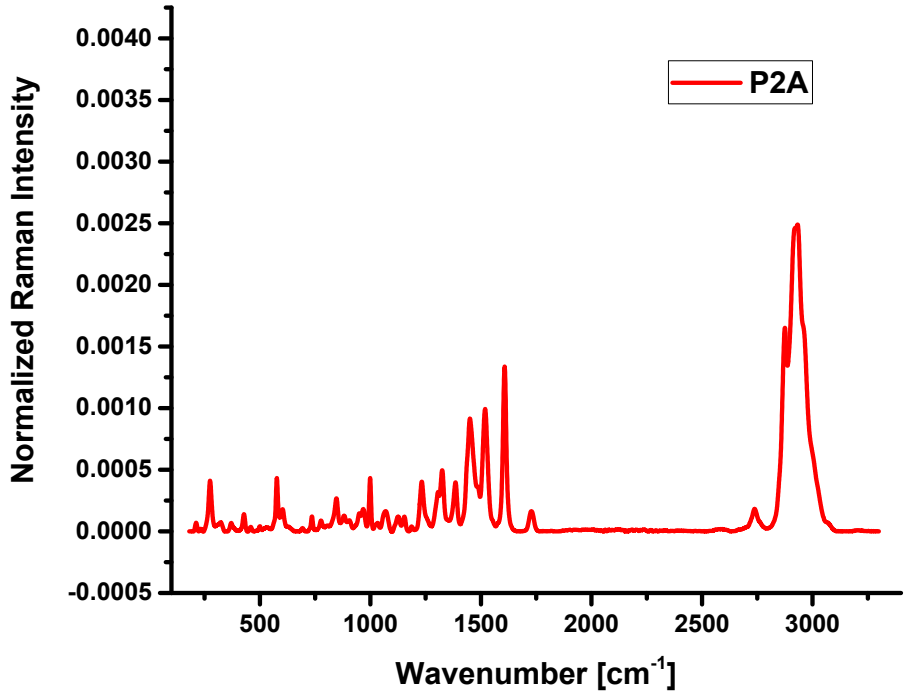

*Figure S 22: Raman spectrum of the polymer **P2A**. Band assignment 3069 (vw, ν(=C-H)), 2998 (w, ν(C-H)), 2958 (s, ν(C-H)), 2932 (vs, ν(C-H)), 2920 (vs, ν(C-H)), 2874 (s, ν(C-H)), 2739 (vw, ν(C-H)), 1729 (vw, ν(C=O)), 1608 (m, ν(C=C)), 1576 (vw, ν(C=C)), 1554 (vw, ν(C=C)), 1520 (m, ν(C=C)), 1488 (sh, δ(C-H)), 1450 (w, δ(C-H)), 1438 (sh, δ(C-H)), 1386 (vw), 1325 (vw), 1306 (vw), 1232 (vw), 1187 (vw), 1154 (vw), 1126 (vw), 1109 (vw), 1068 (vw), 1034 (vw), 1022 (vw), 999 (vw, ring breath phenyl), 968 (vw), 950 (vw), 905 (vw), 882 (vw), 846 (vw), 805 (vw), 777 (vw), 735 (vw), 694 (vw), 603 (vw), 577 (vw, ring breath mesityl), 565 (vw), 500 (vw), 458 (vw), 428 (vw), 371 (vw), 323 (vw), 275 (vw, ν(C-I)), 233 (vw), 212 (vw) cm^{-1}.*

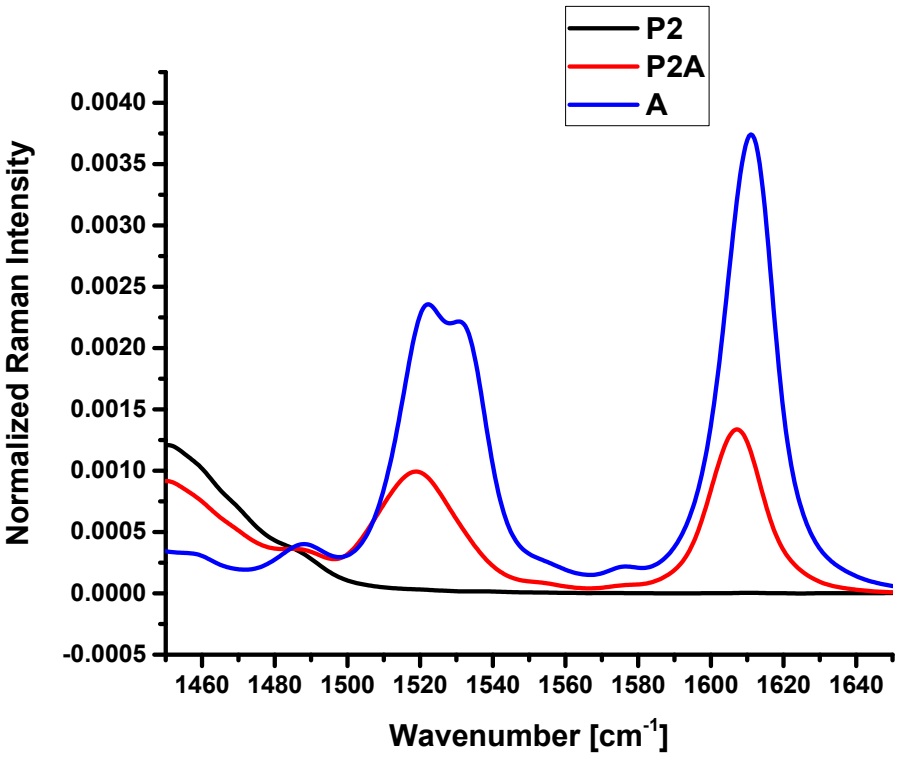

*Figure S 23: Excerpt of the Raman spectra of **P2**, **P2A** and **A**.*

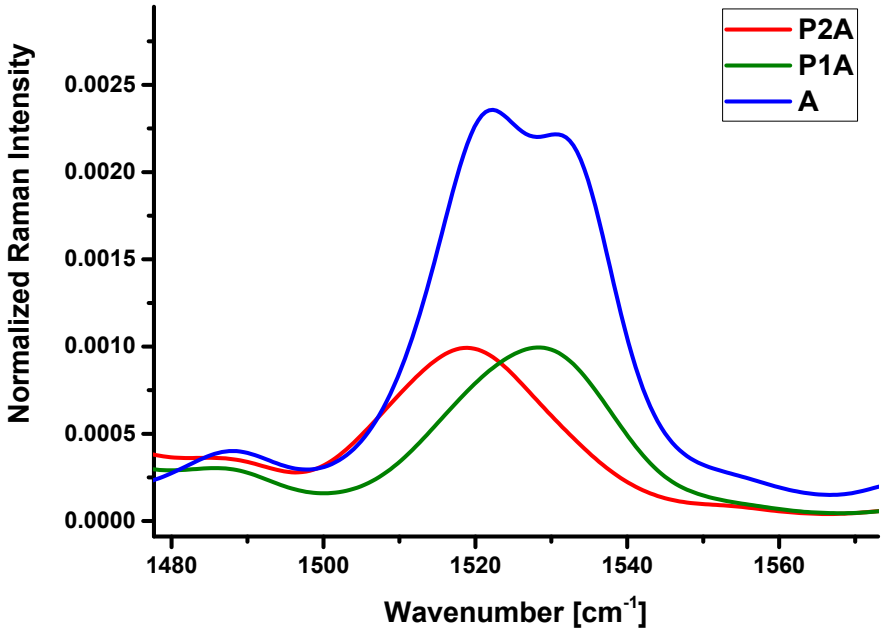

*Figure S 24: Excerpt of the Raman spectra of **P2A**, **P1A** and **A**.*

9. Nanointendation

Table S 6: Depth-sensing indentation (DSI) results (combined results from two measuring areas of the same sample).

		Reduced modulus E_r [c),d)]		Hardness [c),d)]		Indentation modulus E_i [e)]	
Sample	**M.-points**	**Average [GPa]**	**Standard deviation [GPa]**	**Average [GPa]**	**Standard deviation [GPa]**	**Average [GPa]**	**Standard deviation [GPa]**
P1 [a)]	32	1.528	0.022	0.049	0.001	1.285	0.019
P2 [b)]	30	0.315	0.004	0.007	0.001	0.265	0.003
P2A [a)]	32	1.590	0.041	0.054	0.004	1.338	0.034
P2B [a)]	26	0.470	0.090	0.008	0.002	0.395	0.075
P1A [a)]	32	1.149	0.020	0.042	0.002	0.966	0.016

[a)] Measurements were repeated in two measuring areas with sixteen maximum loads in a 4 × 4 array, increasing in steps of 100 µN from 100 to 1600 µN or [b)] in steps of 50 µN from 100 to 850 µN. Values are averaged, measurements outside the area function limits were excluded. [c)] The depth-sensing indentation (DSI) was conducted at ambient conditions at 23.8±0.4 °C and 17.0±5.5% relative humidity (RH). [d)] For quasi-static testing, a 5 s loading, 30 s hold at maximum load, and 5 s unloading profile was applied. [e)] From the reduced modulus E_r, the indentation modulus E_i was calculated using the analysis method proposed by Oliver and Pharr, using the elastic modulus and Poisson's ratio of the diamond indenter, 1140 GPa and 0.07, respectively, and a Poisson's ratio of 0.4 for the polymeric material.[3]

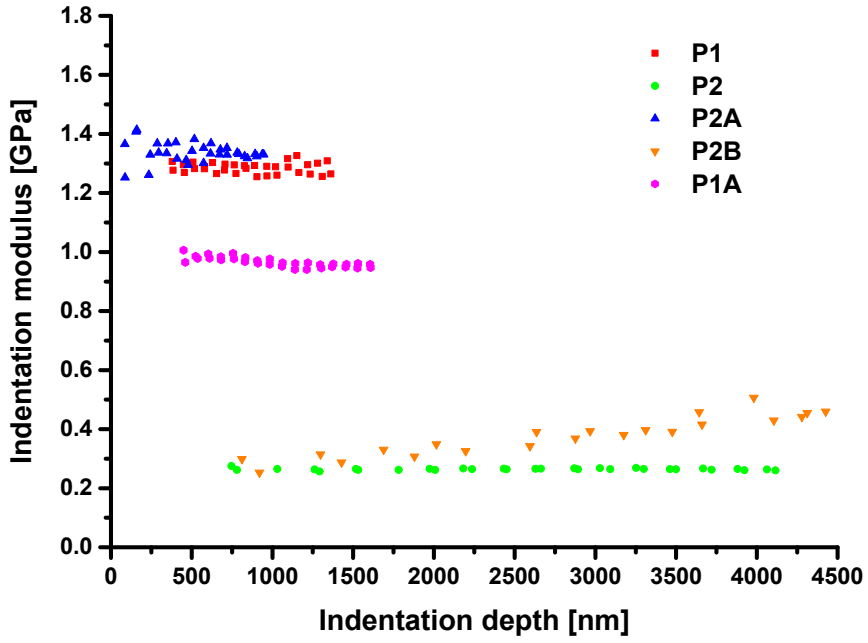

*Figure S 25: Indentation modulus for the polymers **P1**, **P2** and the polymer networks **P1A**, **P2A** and **P2B**.*

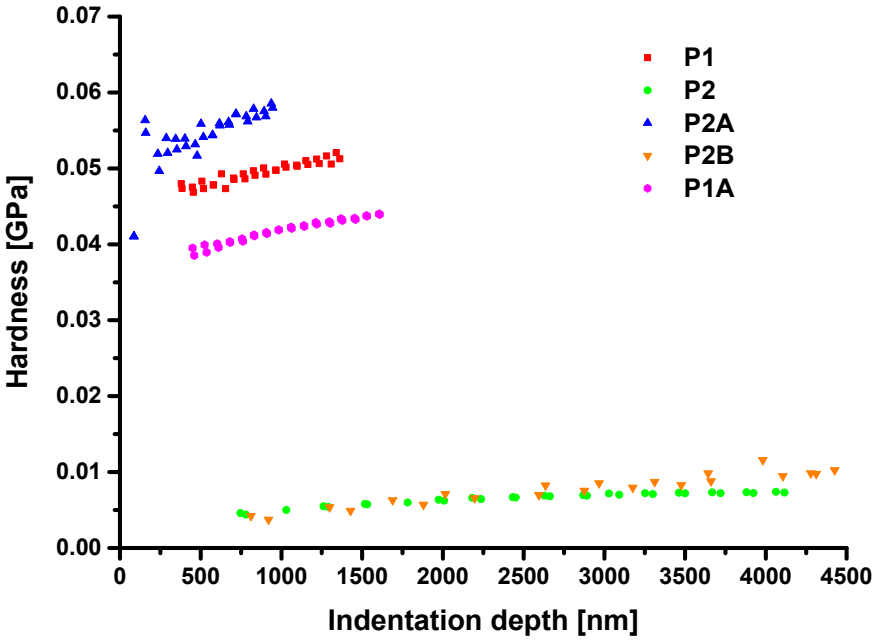

*Figure S 26: Hardness for the polymers **P1**, **P2** and the polymer networks **P1A**, **P2A** and **P2B**.*

10. Isothermal titration calorimetry (ITC)

Table S 7: Experimental setup for ITC measurements.

Cell		Syringe		K [M^{-1}]	ΔG [kJ mol^{-1}]	ΔH [kJ mol^{-1}]	$T\Delta S$ [kJ mol^{-1}]	N	H:G ratio
Species	c [mM]	Species	c [mM]						
A	2	Br^-	28	2.76×10^3	−20.0	−25.1	−5.1	1.78	1:2
B	2	Br^-	28	-[a]	-	-	-	-	-
R1	3	Br^-	27	2.22×10^3	−19.4	−24.5	−5.1	1.00	1:1

[a] No sufficient heat effect was observed in the ITC measurement.

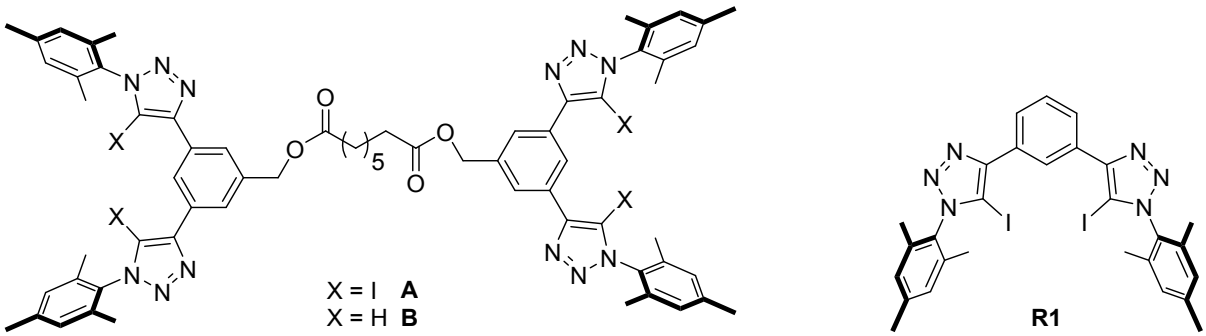

Figure S 27: Schematic representation of the chemical structures of the receptors for ITC measurements.

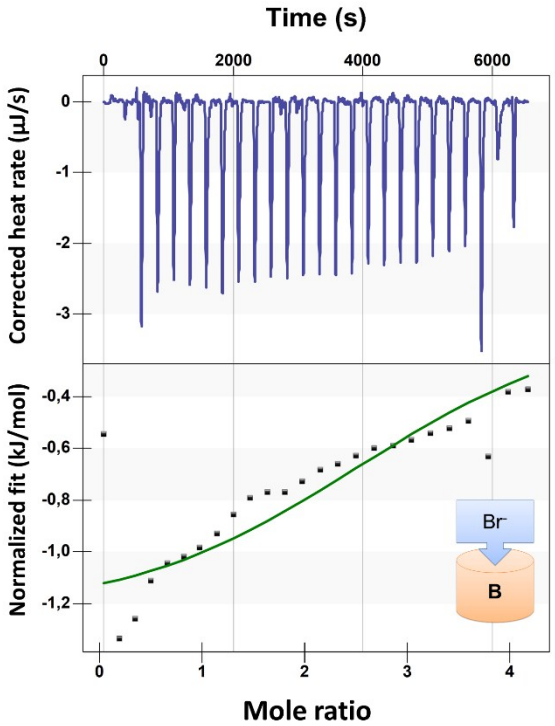

*Figure S 28: ITC titration data of receptor **B** (2 mM, in cell) with Bu_4NBr (28 mM, in syringe) in THF at 303 K.*

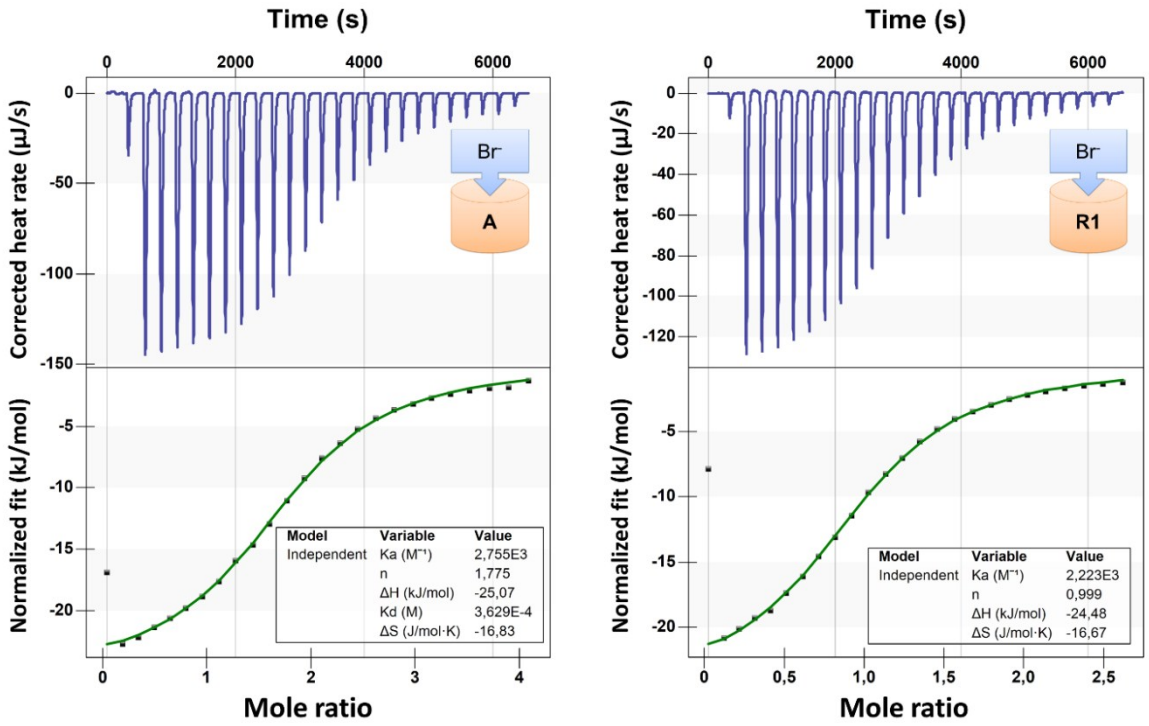

*Figure S 29: ITC titration data of (left) receptor **A** (2 mM, in cell) with Bu_4NBr (28 mM, in syringe) and (right) **R1** (3 mM, in cell) with Bu_4NBr (27 mM, in syringe) in THF at 303 K.*

11. Healing experiments

Table S 8: Summary of the healing experiment (color code: red = no healing, yellow = partial healing, green = healing).

Sample Name	Linker	Counter cation	100 °C
P1	-	-	3.5 h
P2	-	NBu_4^+	3.5 h
P2A	**A**	NBu_4^+	3.5 h
P2B	**B**	NBu_4^+	3.5 h
P1A	**A**	-	3.5 h

P1

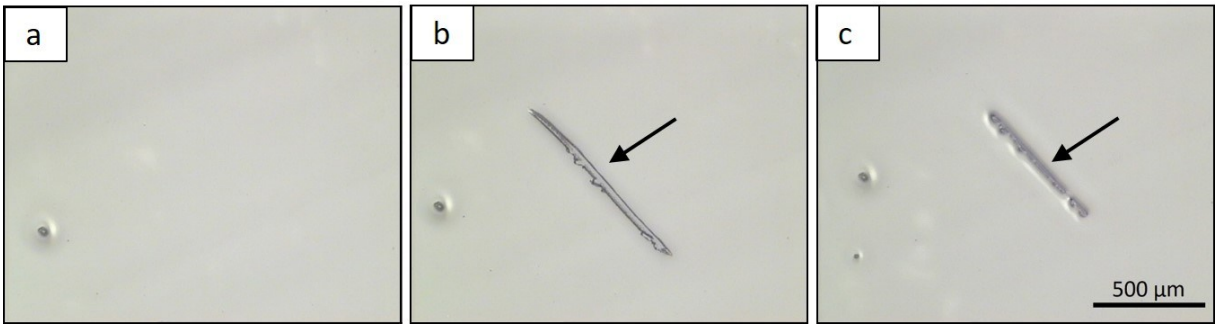

*Figure S 30: Healing experiments of **P1**. a) Film without scratch, b) scratch and c) scratch after 3.5 h at 100 °C.*

P2

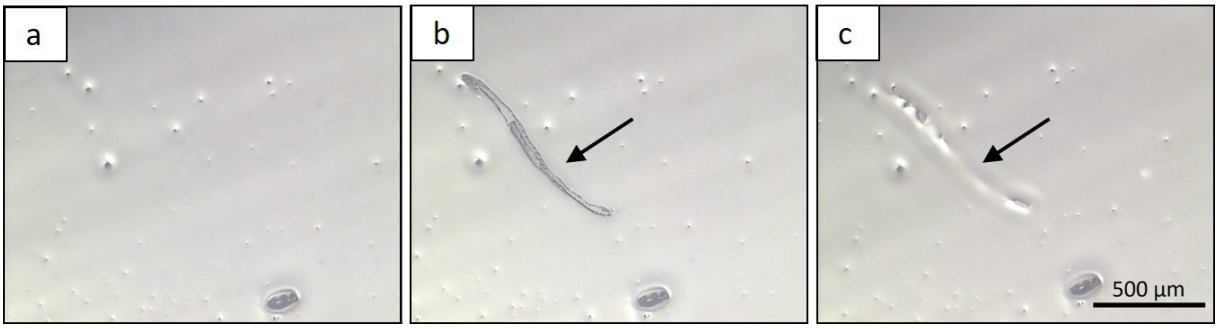

*Figure S 31: Healing experiments of **P2**. a) Film without scratch, b) scratch and c) scratch after 3.5 h at 100 °C.*

P2A

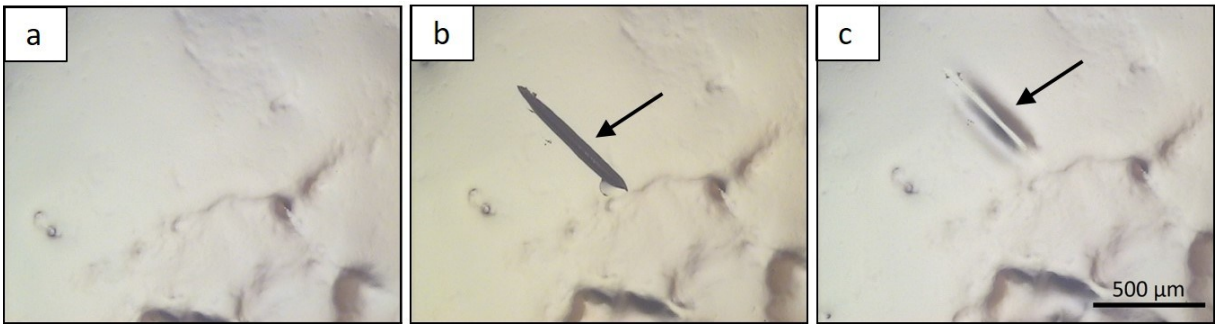

*Figure S 32: Healing experiments of **P2A**. a) Film without scratch, b) scratch and c) scratch after 3.5 h at 100 °C.*

P2B

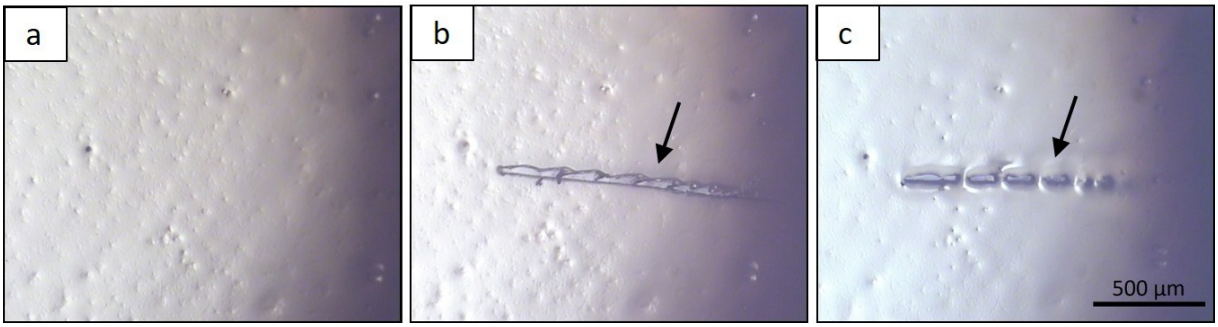

*Figure S 33: Healing experiments of **P2B**. a) Film without scratch, b) scratch and c) scratch after 3.5 h at 100 °C.*

P1A

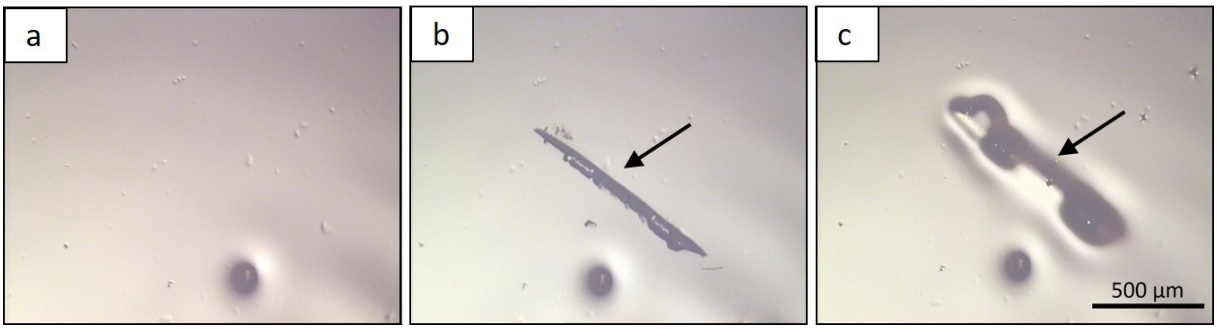

*Figure S 34: Healing experiments of **P1A**. a) Film without scratch, b) scratch and c) scratch after 3.5 h at 100 °C.*

Table S 9: Quantification of the healing efficiency of the most relevant samples by analysis of the images from microscopy studies.

Sample Name	Linker	Counter cation	100 °C	Healing efficiency
P2	-	NBu_4^+	3.5 h	86%
P2A	**A**	NBu_4^+	3.5 h	80%
P2B	**B**	NBu_4^+	3.5 h	63%

The quantification of the healing was performed by analysis of the microscopy images shown above (Figure S 31 to S 33). The software ImageJ was utilized to identify the surface areas of the scratch and the undamaged film, respectively.[4] After binarization of the resulting images, the relative areas of the scratch before and after temperature treatment were calculated. The healing efficiency was calculated from the corresponding ratio of the damaged areas as follows:

$$\% \text{ Scratch healing} = \left(1 - \frac{A_t}{A_i}\right) \times 100$$

A_t = surface area of the scratch after healing

A_i = initial scratch area

12. References

1 R. Tepper, S. Bode, R. Geitner, M. Jager, H. Gorls, J. Vitz, B. Dietzek, M. Schmitt, J. Popp, M. D. Hager and U. S. Schubert, *Angew. Chem. Int. Ed.*, 2017, **56**, 4047–4051.

2 J. Dahlke, R. K. Bose, S. Zechel, S. J. Garcia, S. van der Zwaag, M. D. Hager and U. S. Schubert, *Macromol. Chem. Phys.*, 2017, **218**, 1700340.

3 W. C. Oliver and G. M. Pharr, *J. Mater. Res.*, 1992, **7**, 1564–1583.

4 R. K. Bose, M. Enke, A. M. Grande, S. Zechel, F. H. Schacher, M. D. Hager, S. J. Garcia, U. S. Schubert and S. van der Zwaag, *Eur. Polym. J.*, 2017, **93**, 417–427.